Polym. Bull. (2012) 68:829–845
DOI 10.1007/s00289-011-0646-1

ORIGINAL PAPER

Phosphonate-functionalized polyfluorene and its application in organic optoelectronic devices

Baohua Zhang · Zhiyuan Xie · Lixiang Wang

Received: 21 September 2011 / Accepted: 2 October 2011 / Published online: 15 October 2011

Abstract Conjugated polar polymers, in which the conjugated backbones are chemically anchored with functional polar side groups, can be processed with water/alcohol solvents, and thus multilayered device architectures can be easily realized via sequential solution processing of the toluene-soluble emissive polymer and alcohol-soluble electron-transporting polymer without intermixing. Regarding their use in organic optoelectronic devices, the success in achieving efficient charge injection and intimate contact between metal electrodes and organic semiconductors is very vital for enhancing the device performance. In this short review, it gives a brief review to neutral alcohol-soluble phosphonate-functionalized polyfluorene, mainly concerning the electronic structure at the phosphonate-functionalized polyfluorene/aluminum cathode interface and its successful application in multilayered polymer optoelectronic devices including polymer light-emitting diodes and polymer solar cells.

Keywords Conjugated polymer · Phosphonate group · Interfacial electronic structure · Optoelectronic devices

Introduction

Solution-processible polymer optoelectronic devices, such as polymer light-emitting diodes (PLEDs) [1, 2] and polymer solar cells (PSCs) [3], have recently received great attention due to the cost-efficient fabrication from solution such as inkjet printing and reel-to-reel coating as well as the possibility to achieve high device performance without using complicated device architectures. For achieving high

B. Zhang · Z. Xie (✉) · L. Wang
State Key Laboratory of Polymer Physics and Chemistry, Changchun Institute of Applied Chemistry, Chinese Academy of Sciences, Changchun 130022, People's Republic of China
e-mail: xiezy_n@ciac.jl.cn

device performance, multilayered device structures are always needed since the simple sandwich structure cannot meet relevant device physics considerations. The application of anode or cathode interfacial layers can effectively solve exciton quenching and bipolar charge balance/confinement problems in polymer optoelectronic devices [4]. Unfortunately, owing to the similar solubility of the polymer optoelectronic materials in common organic solvents, interfacial mixing problem alway exists while depositing the multilayered polymer films via sequential solution processing, which is exceedingly harmful to the device performance. Many strategies such as using "orthogonal"solvents [5, 6] or crosslinking methodology [7–9] have been developed to solve this obstacle, and thus high-performance multilayered optoelectronic devices have been obtained.

Conjugated polar polymers (CPPs), in which the electronically delocalized backbones are modified with functional polar side groups, are soluble in environmentally friendly water/alcohol solvents (meet the demands of "orthogonal" solvent strategy for multilayered device assembly) and thus have wide applications in optoelectronic devices especially as the electrode interfacial layer. Recent progress in PLEDs and PSCs with CPP buffer layers indicates that the distinct roles with these interfacial materials depend on their advantages at tailoring interfacial electronic structure that forms favorable interfacial energy level alignments to enhance charge injection or collection [10–12]. The growing recognition discloses that it is the peculiar pedant polar group that tailors the interfacial electronic level while the conjugated backbone remains the charge-transport capability. For example, on the origin of efficient electron injection from stable metal electrodes (e.g., Au, Ag, or Al) to CPP interfacial layer, intrinsic dipoles and/or reactivity of polar groups in the vicinity of CPP/cathode metal interfaces are mainly involved [11, 13]. Although, the effectiveness of CPPs is reported, the successful examples are scarce, in which the pendent groups mainly include amino-/amino derivative-, phosphonate-, and oxide-containing groups [10, 13–16]. It should be mentioned that, analogous to CPPs, conjugated polyelectrolytes (CPEs), in which the polar groups are charged ions instead, are alternatively developed with the similar molecular structure designs and applications [17]. However, the prevalent mechanism arising from electrical-field-induced redistribution of the ions at CPEs/electrode interfaces would cause slow optoelectronic response (even at min. level) under bias [18], which limits their applications.

In this short review, we will give a brief review to neutral alcohol-soluble phosphonate-functionalized polyfluorene (PF-EP). The PF-EP was first developed as a chemical sensor material by our group. We successfully applied it as a cathode buffer layer in multilayered PLEDs and PSCs and the device performance was dramatically improved with high work-function Al cathode. The electronic structure and the origin of efficient electron injection at the PF-EP/Al interface were discussed in detail. It should be emphasized that CPPs and CPEs have been developed quickly in recent years and show great potential applications not only in PLEDs and PSCs [15–17, 19], but also in chemical sensors and biology field [20, 21].

Structure and photophysical properties of PF-EP

Figure 1 shows the chemical structure of PF-EP polymer. As depicted, the only difference relative to poly(9,9-dialkylfluorene)s (PFs) is the attachment of phosphonate groups at the end of the alkyl side chains of PFs. PF-EP is soluble in most of common organic solvents, such as tetrahydrofuran (THF), toluene, dimethylformamide (DMF), chloroform ($CHCl_3$), and dimethyl sulfoxide (DMSO). Especially, it is also highly soluble in methanol, ethanol, and acetone. The solubility of PF-EP in ethanol is over 10 mg/mL. The result from cyclic voltammetry measurement shows that the highest occupied molecular orbit (HOMO) and lowest unoccupied molecular orbital (LUMO) energy levels of PF-EP locate at −5.5 and −2.2 eV, respectively [14], 0.3 eV higher than the HOMO level of PF analog, which is analogous to other reported fluorene-based polyelectrolyte [22]. Figure 2 shows the absorption and photoluminescent (PL) spectra of PF-EP in different solutions and in films. The absorption and PL spectra of PF-EP show the same characteristic features of PF counterpart, implying the little influence of the pendant phosphonate groups on the π-delocalized PF backbones. As shown in Fig. 2, the absorption maximum of PF-EP in chloroform, ethanol, DMF, and DMSO is at 392, 401, 400, and 406 nm, while the emission bands are peaked at 418, 422, 423, and 424 nm with vibronic shoulder around 442, 436, 445, and 438 nm, respectively. Since, no aggregation absorption or excimer emission was observed; we attribute this red shift to enhanced chain conjugation driven by strong interaction between phosphonate groups and solvent molecules in polar solvents. The PF-EP film cast from ethanol solution shows a 3–9 nm red shift with major peak at 437 nm and two clear vibronic shoulders at 460 and 490 nm. It may be attributed to improved intrachain order or longer effective conjugation length of PF-EP [14].

Efficient PLEDs with high work-function metal cathode

The electroluminescent (EL) property of PF-EP was investigated with different metals as the cathode in a device configuration of ITO/poly(vinylcarbazole) (PVK, 25 nm, spin-coated from $CHCl_3$ solution)/PF-EP (60 nm, spin-coated from ethanol

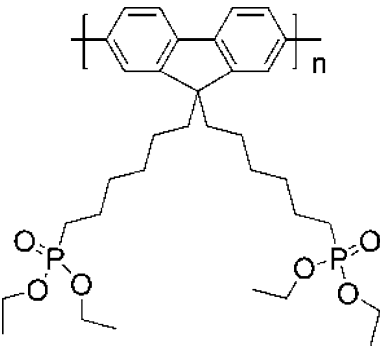

Fig. 1 Chemical structure of PF-EP

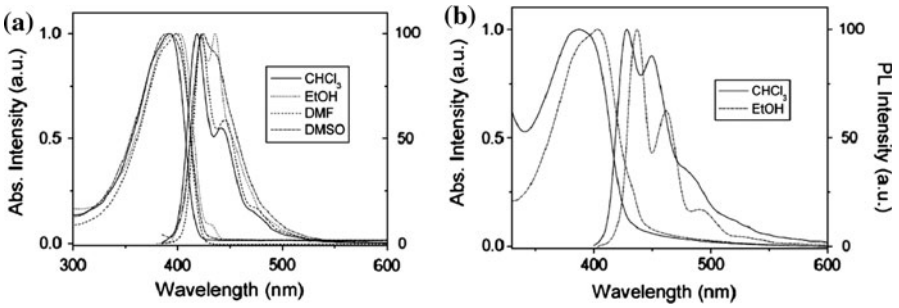

Fig. 2 Absorption and PL spectra of PF-EP in $CHCl_3$, EtOH, DMF, and DMSO solutions (**a**) and in films spin-coated from $CHCl_3$ and EtOH (**b**). Reprinted with permission from [14]. Copyright (2005) American Chemical Society

solution)/metal cathode. The cathodes of Al (100 nm), Ca (10 nm)/Al (100 nm), Mg (10 nm)/Al (100 nm), and Ag (10 nm)/Al (100 nm) were used for comparison [23]. The PLED performance is summarized in Table 1. As can be seen, the best device performance is obtained by using Al cathode. The maximum luminous efficiency reaches to 4.0 cd/A along with the Commission Internationale del'Eclairage (C.I.E.) coordinates of (0.18, 0.14), indicating that PF-EP is an efficient blue emitter. Since, the LUMO level of PF-EP is −2.2 eV, the efficient electron injection and high light-emitting efficiency are supposed to be achieved with low-work-function metals such as Ca cathode according to energy level diagram consideration with Schottky–Mott model [24]. In this case, although the work function of Ca is much lower than that of Al, the PLED with high work-function Al cathode demonstrates a much lower turn-on voltage and higher light-emitting efficiency. This suggests that the combination of PF-EP and Al metal cathode does realize more efficient electron injection, as further confirmed by electron-only devices with these metal cathodes [23]. In the following section, it is further identified that the phosphonate groups attached on the PF backbone play a crucial role in realizing efficient electron injection at the PF-EP/Al interface. The main cause is ascribed to the favorable interfacial dipoles and in situ coordination interaction between functional phosphonate groups and topmost Al atoms [11].

Table 1 Summary of the device performance of PLEDs with different cathodes [23]

Architectures	V_{on} (V)	B (Max.) (cd/m^2)	LE (Max.) (cd/A)	EL peak (nm)	C.I.E.[a] (x, y)
ITO/PVK/PF-EP/Ca/Al	5.6	3910	1.6	–	–
ITO/PVK/PF-EP/Mg/Al	6.0	1125	1.1	–	–
ITO/PVK/PF-EP/Al	4.6	3668	4.0	436/460/490	0.18, 0.15
ITO/PVK/PF-EP/Ag/Al	6.9	1509	1.0	–	–

[a] At a luminance of 500 cd/m^2

Efficient multilayered PLEDs with PF-EP/Al cathode

To achieve highly efficient and stable PLEDs, a multilayered device configuration of a hole injection/transport layer (HIL/HTL)/an emissive layer (EML)/an electron transport/injection layer (ETL/EIL) is typically required to enhance charge injection and balance bipolar transport [4, 5]. Compared to the commonly used low-work-function metals, such as Ca, the employment of water/alcohol-soluble CPPs or CPEs in conjunction with stable metal cathodes, such as Al, not only eliminates the interface degradation by reaction with trace oxygen and moisture [25, 26], but also prevents the excitons from quenching at the cathode interfaces [27, 28]. PF-EP was successfully used in PLEDs as ETL/EIL in conjunction with stable Al metal cathode, and the device performance was greatly enhanced. The origin of the efficient electron injection at the PF-EP/Al interface was further verified by using ultraviolet and X-ray photoelectron spectroscopy (UPS/XPS) measurements.

Figure 3 shows the device structure of the multilayered PLEDs and the emissive polymers used for this study. The device structure consisted of ITO/PEDOT:PSS (45 nm)/EML (110 nm)/PF-EP (30 nm)/Al (100 nm). The "orthogonal" solvents used for sequential spin-coating of the PEDOT:PSS, EML, and PF-EP layer are water, toluene, and alcohol, respectively. There is no inter-diffusion between EML and PF-EP as further confirmed by the clear interface formation from the cross-section scanning electron microscope images [29]. Blue, green, and red PLEDs were fabricated with PF-EP/Al as the cathode and with PFO, GPFO, RPFO as EML, respectively. The corresponding control devices with Ca/Al cathodes were also prepared for comparison. As shown in Table 2, all PLEDs with PF-EP/Al cathode exhibit superior performance compared to the control PLEDs. For example, by the replacement of Ca/Al with PF-EP/Al, the peak luminous efficiency (LE) of the blue, green, and red PLEDs are promoted from 2.78, 7.97, and 4.39 cd/A to 5.02, 15.0, and 7.01 cd/A, respectively. The EL spectra of these PLEDs with PF-EP/Al cathode solely stem from the emissive layer, indicating that the exciton recombination region is restricted within the EML and apart from the metal cathode. Thus, the possible exciton quenching at the cathode is avoided.

To comprehensively estimate the validity of the PF-EP/Al cathode in PLEDs, a series of GPFO-based PLEDs with different cathode structures were compared and their device performance is presented in Fig. 4. As can be seen in Fig. 4, the device with PF-EP/Al cathode exhibits an efficiency of 15.0 cd/A, much higher than 12.5, 7.8 and 0.3 cd/A for the devices with Ba/Al, Ca/Al, and Al cathodes, respectively. The current density (J)–voltage (V) curves of these PLEDs are also shown in Fig. 4. At same driving voltages, the device with PF-EP/Al exhibits the largest current density and luminance among these PLEDs, indicating that the PF-EP/Al structure realizes more efficient electron injection than that from Ba/Al or Ca/Al cathode. These proofs further reinforce the aforementioned view that both the efficient electron injection (even better than low-work-function Ca and Ba cathodes) and prevention of exciton quenching at the cathode interface do favor realizing superior performance of the multilayer PLEDs.

The UPS/XPS measurements were carried out to explore the origin of the efficient electron injection at PF-EP/Al interface [11]. As shown in Fig. 5, there is a

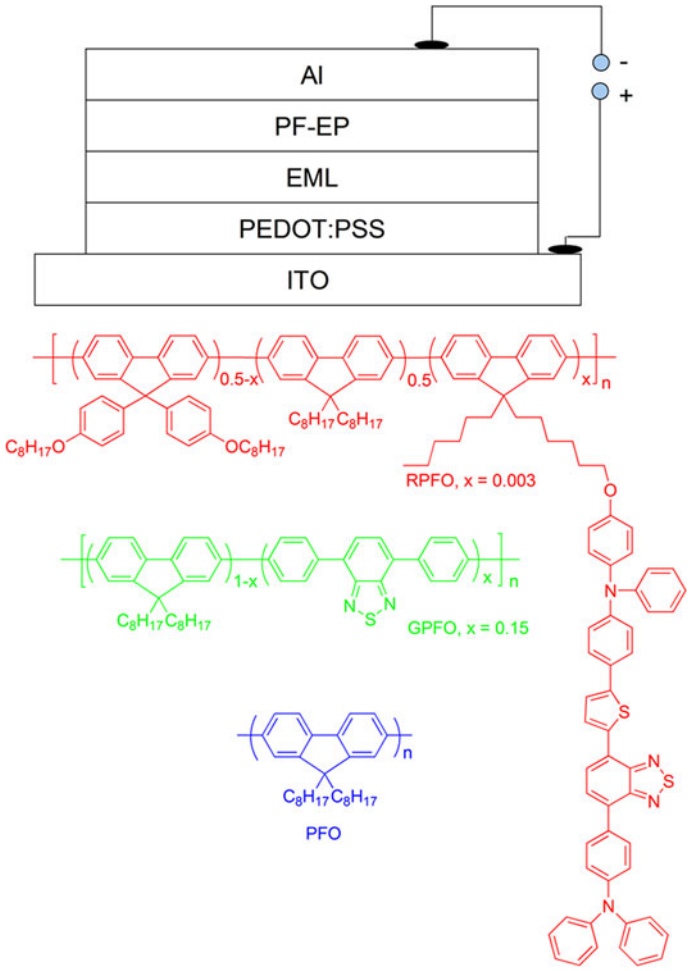

Fig. 3 The architecture of multilayer PLEDs and the chemical structures of RGB polymer RPFO, GPFO and PFO, respectively

Table 2 Summary of the device performance of PLEDs with PF-EP/Al or Ca/Al

EML/cathode	V_{on} (V)	B (Max.) (cd/m^2)	LE (Max.) (cd/A)	PE (Max.) (lm/W)	C.I.E. (x, y)
PFO/Ca/Al	3.7	2125	2.78	2.03	(0.17, 0.13)
PFO/PF-EP/Al	3.5	4603	5.02	4.64	(0.17, 0.15)
GPFO/Ca/Al	6	13780	7.97	2.56	(0.34, 0.61)
GPFO/PF-EP/Al	4.5	15350	15.0	8.27	(0.35, 0.57)
RPFO/Ca/Al	6	5614	4.39	1.72	(0.57, 0.38)
RPFO/PF-EP/Al	5	14980	7.01	3.15	(0.57, 0.39)

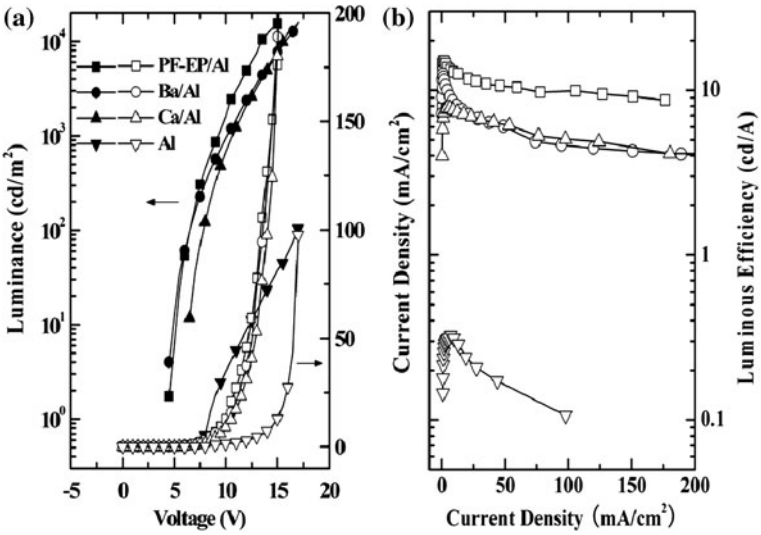

Fig. 4 *J–L–V* (**a**) and LE–*J* (**b**) characteristics of the GPFO-based PLEDs with different cathode structures. Reprinted with permission from [11]. Copyright (2010) American Institute of Physics

0.43 eV interfacial dipole pointing to Al electrode and 0.1 eV band bending at the PF-EP/Al interface. This favorable dipole formation is attributed to the distinct difference in electronegativities of P and O elements in phosphonate groups (2.19 and 3.14, respectively) as stated in Vaynzof and Kahn et al.'s study [30]. As a result, there is $\sim$0.6 eV reduction of electron-injection barrier at the PF-EP/Al interface with respect to the PF/Al interface. The possible interfacial interactions between Al and phosphonate group in PF-EP at PF-EP/Al interface were examined via Ar + ion etching technique to remove the top Al layer gradually. The evolutions of Al 2*p* lines of the Si/PF-EP/Al (10 nm) and Si/PF/Al (10 nm) samples with increased sputtering time are presented in Fig. 6. In addition to the same metallic Al and Al_xO_y peaks (peak a and b, respectively) to the Si/PF/Al sample, the distinct peak c located at 73.3 eV was detected for the Si/PF-EP/Al (10 nm) sample, which originates from the thin Al at the PF-EP/Al interface. It is ascribed to the formation of P–O–Al coordination when hot Al atoms are deposited onto the PF-EP layer in view of the strong coordination capability of P=O bond in phosphonate groups with metals even under moderate conditions [31, 32]. As reported [33–35], such coordination may increase interfacial dipole effect and result in interfacial *n*-type doping of the PF-EP layer at PF-EP/Al interfaces, which contributes to further reduce electron-injection barrier from Al cathode to the PF-EP layer.

Efficient multilayered white PLEDs

Since, the polymer PF-EP simultaneously possesses efficient blue emission and electron-injection property with Al cathode, an efficient all-polymer white PLED

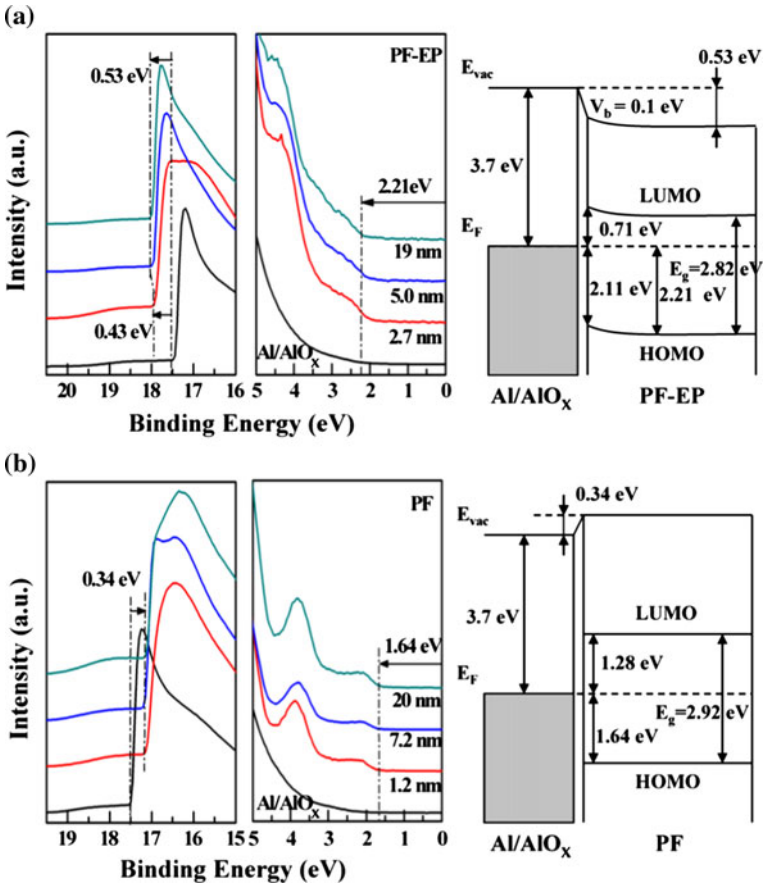

Fig. 5 UPS spectra of **a** Al/PF-EP (varied thickness) and **b** Al/PF (varied thickness) samples and the corresponding energy diagram at the interfaces. Reprinted with permission from [11]. Copyright (2010) American Institute of Physics

with a configuration of ITO/PEDOT: PSS (60 nm)/poly[9,9-din-octylfluorene-co-4,7-bis(4-[*N*-phenyl-*N*-(4-methylphenyl) amino]phenyl)-2,1,3-benzothiadiazole] (PF-BT05) (130 nm)/PF-EP (35 nm)/Al (100 nm) was fabricated [29]. PF-BT05 is a kind of white emissive polymer in which 0.05 mol% orange fluorescent benzothiadiazole moieties are introduced. As shown in Fig. 7, the EL spectra of PF-BT05 (device structure: ITO/PEDOT:PSS/PF-BT05/Ca/Al) cannot realize pure white emission due to the weak blue emission. When the PF-EP is introduced as a blue emitter and electron injector, the PLED shows a pure white emission with balanced blue and orange contributions. The CIE coordinates are improved from (0.42, 0.43) to (0.39, 0.38). In addition, there is also a great improvement in device efficiency from 10.1 to 16.9 cd/A, which is among the highest efficient fluorescent white PLEDs [36, 37]. In this case, considering the combinational EL spectra contribution from both emitters, the exciton recombination zones are certainly

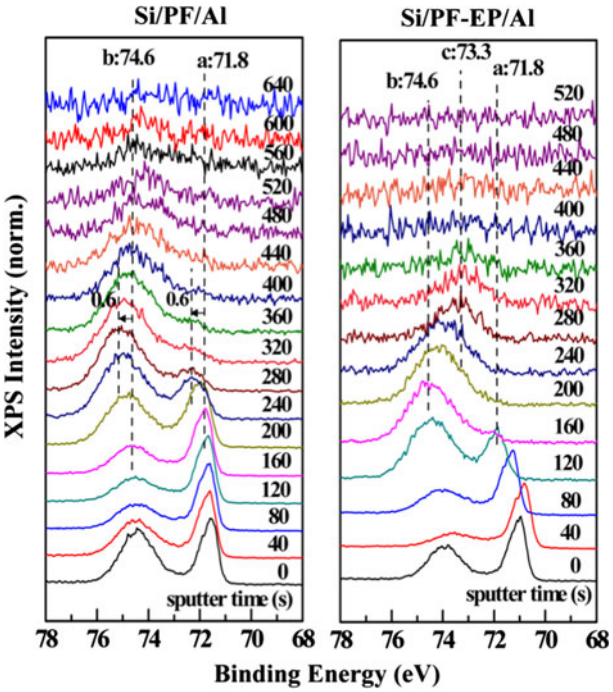

Fig. 6 The evolutions of Al 2*p* core level lines with stepwise etching the Si/PF/Al (10 nm) (*left*) and Si/PF-EP/Al (10 nm) (*right*) samples. Reprinted with permission from [11]. Copyright (2010) American Institute of Physics

confined at the PF-BT05/PF-EP interface and away from the metal cathode. Thus, the exciton quenching at the cathode interface is avoided. It further verified that manipulating the exciton recombination zone near/at the heterojunction interface is an effective pathway to achieve high light-emitting efficiency [38]. It is noted that the PF-EP layer in the device serves as not only an efficient blue fluorescent emitter, but also an efficient electron injector in combination with Al cathode.

Highly efficient three-color fluorescent white PLEDs were also fabricated with a structure of ITO/PEDOT:PSS (50 nm)/WP-B5G5R2 (90 nm)/PF-EP (30 nm)/LiF (1 nm)/Al (100 nm) [39]. Herein, the PF-EP/LiF/Al structure is used as a more efficient electron injector and the mechanism will be explained later. The three-color white single polymer WP-B5G5R2 with 0.05, 0.05, and 0.02 mol% amounts of blue, green, and red fluorescent chromophores being covalently anchored onto side chains of PF backbone is used as the EML [40]. As shown in Fig. 8, significant improvement of the device performance is achieved by using PF-EP/LiF/Al cathode. 98, 150, and 128% increase of the peak LE, power efficiency (PE), and luminance to 12.5 cd/A, 10.5 lm/W, and 37800 cd/m^2 are achieved, respectively, as compared to 6.3 cd/A, 4.2 lm/W, and 16610 cd/m^2 of the control device with Ca/Al cathode. When the EML layer is subjected to thermal annealing, the device performance is further improved due to the formation of efficient blue α-phase crystalline PF and balanced charge transport [39, 41, 42]. The detailed performance

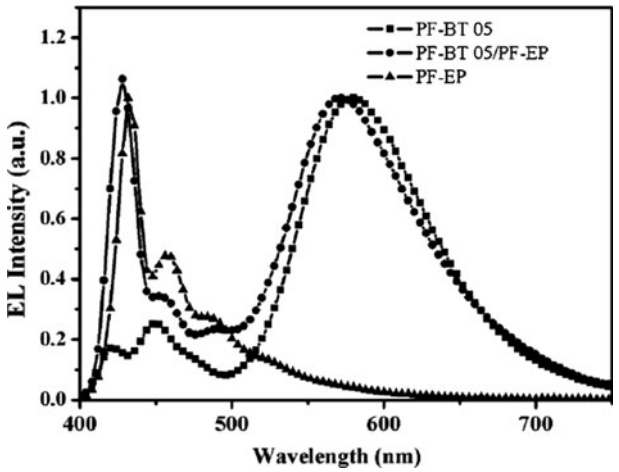

Fig. 7 EL spectra of the PLEDs with structures of ITO/60 nm PEDOT:PSS/130 nm PF-BT05/Ca/Al, ITO/60 nm PEDOT:PSS/130 nm PF-BT05/35 nm PF-EP/Al, and ITO/60 nm PEDOT:PSS/100 nm PF-EP/Al. Reprinted with permission from [29]. Copyright (2007) American Institute of Physics

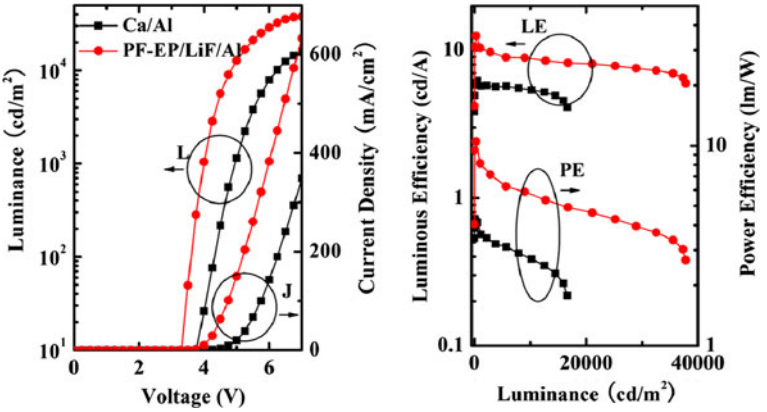

Fig. 8 Device performance of the white PLEDs with cathode structures of Ca/Al and PF-EP/LiF/Al

is summarized in Table 3. For the PLEDs with PF-EP/LiF/Al cathode, no blue emission from PF-EP is observed indicating that the exciton zone is confined in the EML due to efficient electron injection at PF-EP/LiF/Al interfaces. According to the literatures [27, 28, 33], diffusion of the metal atoms of cathode into EML will severely influence device efficiencies. Herein, the 30-nm-thick PF-EP layer serves as a buffer layer and prevents the metal atoms from diffusing into the EML layer. The second reason for the performance enhancement of the PLEDs with PF-EP/LiF/Al stems from the more efficient electron injection facilitating the balance of bipolar carriers within the EML in view of the hole-dominated mobility of PF backbones and the comparable hole/electron-injection barriers for the control device with

Table 3 Summary of the device performance for the WP-B5G5R2-based white PLEDs with different cathodes [39]

Conditions	LE (cd A^{-1})[a]	PE (lm W^{-1})[a]	EQE (%)[a]	Brightness (cd m^{-2})[a]	LE (cd A^{-1})[b]	PE (lm W^{-1})[b]	EQE (%)[b]	CIE (x, y)[b]	CRI[b]
EML (pristine)/Ca/Al	6.3	4.2	2.8	16610	6.2	4.1	2.8	(0.35, 0.39)	88
EML (pristine)/PF-EP/LiF/Al	12.5	10.5	5.2	37810	11.6	9.5	4.8	(0.38, 0.45)	80
EML (120 °C)/PF-EP/LiF/Al	15.4	11.4	6.7	46830	14.2	10.4	6.2	(0.37, 0.42)	85

Reprinted with the permission from [39]. Copyright 2010 Wiley-VCH Verlag Gmbh & Co. KGaA

[a] Peak values

[b] The values measured at a luminance of 500 cd m^{-2}

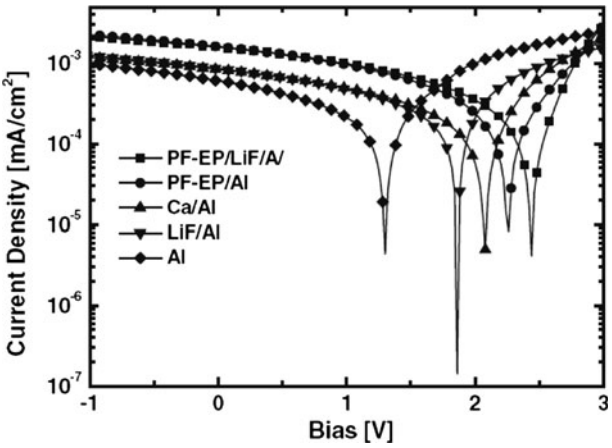

Fig. 9 Photovoltaic characteristics of the devices with a structure of ITO/PEDOT:PSS/EML/different cathodes. Reprinted with the permission from [39]. Copyright (2010) Wiley-VCH Verlag Gmbh & Co. KGaA

Ca/Al [39]. As illustrated below, the electron injection from the PF-EP/LiF/Al is significantly superior to that from the Ca/Al and the PF-EP/Al cathode.

Photovoltaic characteristics of devices with a series of cathode structures were investigated to confirm the effectiveness of electron injection from PF-EP/LiF/Al. As shown in Fig. 9, the open-circuit voltage (V_{OC}) of the devices with different cathodes of the PF-EP/LiF/Al, PF-EP/Al, Ca/Al, LiF/Al, and Al are 2.43, 2.24, 2.08, 1.86, and 1.30 V, respectively, indicating that the PF-EP/LiF/Al structure possesses the lowest effective work function among these cathodes and is the best electron injector. This conclusion was also confirmed by the comparisons of *J*–*V* characteristics of the corresponding electron-only devices with these cathode structures [39]. It is the fact that the insertion of the ultra-thin LiF layer in the vicinity of PF-EP/Al further enhances its electron-injection ability. Considering the strong coordination ability of phosphonate groups mentioned above [31, 32], similar mechanism to the state-of-the-art Alq_3/LiF/Al interfaces is considered to be the main reason [33, 43]. It is that LiF dissociates at the PF-EP/Al interface and thus Li-doping of the PF-EP at the topmost surface are responsible for the more efficient electron injection.

We stress that it is distinctly different for the cathode structures of PF-EP/LiF/Al and PF-EP/Al. The PF-EP layer in both structures is at least 30-nm-thick to prevent Al atoms from penetrating into the EML in PLEDs. Despite the effectiveness of electron injection from PF-EP/Al (superior to Ba, Ca, etc.) [11], the devices using PF-EP/Al still exist blue emission from the PF-EP layer, especially at high biases. On the contrary, the PF-EP/LiF/Al structure fully avoids this phenomenon owing to the more efficient electron injection and indeed serves as a much better electron injector in PLEDs. Very recently, this structure has been widely used in other new emissive polymers to enhance their EL performance significantly [44, 45].

Application of PF-EP as a buffer layer in PSCs

PSCs based on a blend of semiconducting polymer and fullerene derivatives have become a highlight research area in view of the combined attraction of cost-effective, mechanical flexibility, and the compatibility with large-area roll-to-roll coating techniques [3]. For a typical device configuration of ITO/PEDOT:PSS/active layer/Al, the diffusion of Al atoms into the active layer is unavoided and would result in a large leakage current and low shunt resistance (R_{SH}), thereby limiting the power conversion efficiency (PCE) of the PSCs. To solve this problem, a series of buffer layers, including LiF [46], CaO [47], poly(ethylene oxide) (PEO) [48] etc., are inserted between the active layer and Al cathode. However, owing to the limitation of their insulating properties, these buffer layers used in PSCs are too thin (within 1–2 nm) to fully prohibit metal diffusion from occurring at the cathode interface.

Alternatively, we used the alcohol-soluble PF-EP as the cathode buffer layer in PSCs and the device performance was dramatically enhanced [12]. Compared to the aforementioned insulating interfacial materials, the PF-EP buffer layer can be thick enough (5–10 nm) without suffering from sharp increase of series resistance (R_S) because of its intrinsic charge-transport ability. The studied photovoltaic system is the blend of regioregular(3-hexylthiophene) (P3HT): [6,6]-phenyl-C_{61}-butyric acid methyl ester (PCBM). When the 5-nm-thick PF-EP buffer layer was introduced between the P3HT:PCBM(1:0.8) and Al, R_{SH} was increased two orders of magnitude from 30.7 kΩ cm^{-2} to 1.14 MΩ cm^{-2}, V_{OC} was enhanced from 0.45 to 0.64 V, and fill factor was improved from 51 to 59%, thus leading to a PCE of 3.4% (vs. PCE of 2.0% for the control device). Figure 10 shows the dark and illuminated J–V characteristics of the PSCs with Al and PF-EP/Al cathodes. The insertion of 5-nm-thick PF-EP reduces the leakage current by two orders of magnitude. The V_{OC} was also increased by 42% from 0.45 to 0.64 V due to increase of R_{SH}. Furthermore, the PF-EP buffer layer lowers the contact resistance, resulting in a higher short-circuit current (J_{SC}) compared to that of control device. As shown in Fig. 10b, the J_{SC} was further increased from 9.01 to 10.28 mA cm^{-2} after post-annealing treatment since it further effectively reduces the R_S from 10.19 to 6.32 Ω cm^{-2} and therefore results in better charge collection.

Kim and Cao groups [49, 50] reported similar results by using their prototype CPEs as cathode interfacial layer in PSCs with the analog effect, especially increasing the V_{OC} of their PSCs. Very recently, Bazan and co-workers reported a PSC based on a low bandgap donor polymer with PCE as high as 6.5% by using a CPE as a cathode buffer layer [51], further confirming the effectiveness of this strategy in obtaining highly efficient PSCs.

Conclusions

This article provides an overview of the alcohol-soluble phosphonate-containing polyfluorene PF-EP and its application in PLEDs and PSCs as the cathode interfacial layer. Owing to the efficient electron injection from PF-EP/Al and

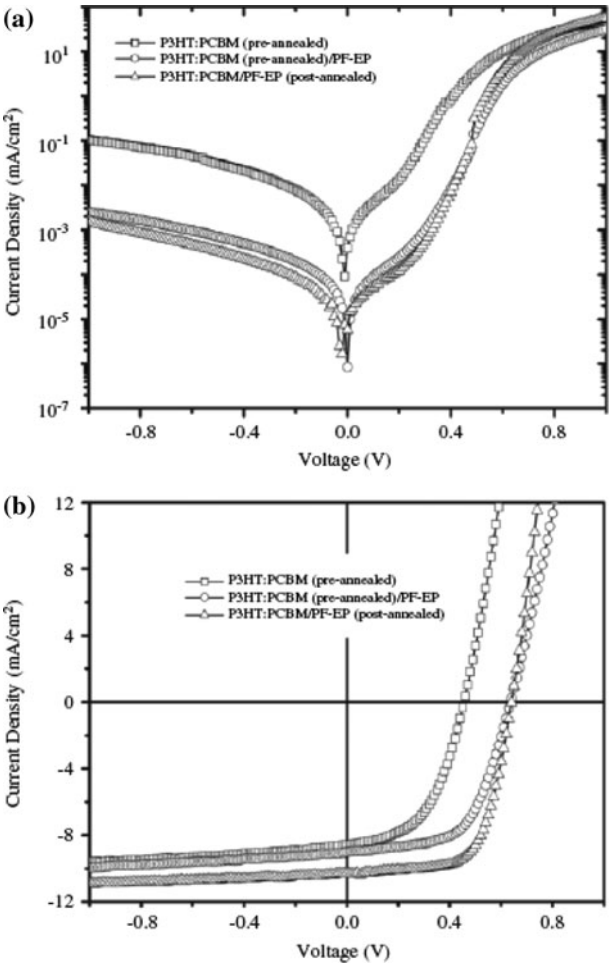

Fig. 10 Dark (**a**) and illuminated (**b**) *J–V* curves of three kinds of P3HT:PCBM blend PV cells under 100 mW cm^{-2} white light illumination: P3HT:PCBM (annealed)/Al (*open squares*); P3HT:PCBM (annealed)/5.0 nm PF-EP/Al (*open circles*); P3HT:PCBM/5.0 nm PF-EP/Al(post-annealed, *open triangles*). Reprinted with the permission from [12]. Copyright (2009) Elsevier

PF-EP/LiF/Al, high-efficiency RGB and white PLEDs with high work-function Al cathode were developed and demonstrated superior device performance with respect to those PLEDs with low-work-function metal cathode (e.g. Ca, Ba). It is confirmed that the favorable interfacial dipoles and intense coordination ability of phosphonate groups at the PF-EP/Al and PF-EP/LiF/Al interfaces account for the efficient electron injection. More importantly, the solution-processed multilayered structure is realized and can effectively prevent metal atoms from diffusion into the emissive layer and avoid exciton quenching at the cathode interface. Recent study by Ye et al. [52] that it is also possible to achieve efficient phosphorescent PLEDs with *n*-type doping PF-EP layer. However, it should be mentioned here that the low triplet level

of PF-EP would limit its application in blue phosphorescent PLEDs. The high electron-mobility and high triplet-level alcohol-soluble polymers with phosphonate group would be a potential high-performance interfacial polymer and possesses more extensive application in organic optoelectronic devices [53].

Acknowledgments The authors acknowledge financial support from the National Natural Science Foundation of China (nos. 60977026, 20834005, and 20921061) and 973 Project of Ministry of Science and Technology of China (2009CB623602, 2009CB930603).

References

1. Wong WY, Ho CL (2009) Heavy metal organometallic electrophosphors derived from multi-component chromophores. Coord Chem Rev 253:1709
2. Reineke S, Lindner F, Schwartz G, Seidler N, Walzer K, Luessem B, Leo K (2009) White organic light-emitting diodes with fluorescent tube efficiency. Nature 459:234
3. Thompson BC, Frechet JMJ (2008) Organic photovoltaics—polymer-fullerene composite solar cells. Angew Chem Int Ed 47:58
4. Meerholz K (2005) Device physics—enlightening solutions. Nature 437:327
5. Gong X, Wang S, Moses D, Bazan GC, Heeger AJ (2005) Multilayer polymer light-emitting diodes: white-light emission with high efficiency. Adv Mater 17:2053
6. Zhang B, Li W, Yang J, Fu Y, Xie Z, Zhang S, Wang L (2009) Performance enhancement of polymer light-emitting diodes by using ultrathin fluorinated polyimide modifying the surface of poly(3,4-ethylene dioxythiophene):poly(styrenesulfonate). J Phys Chem C 113:7898
7. Gather MC, Koehnen A, Falcou A, Becker H, Meerholz K (2007) Solution-processed full-color polymer organic light-emitting diode displays fabricated by direct photolithography. Adv Funct Mater 17:191
8. Png RQ, Chia PJ, Tang JC, Liu B, Sivaramakrishnan S, Zhou M, Khong SH, Chan HSO, Burroughes JH, Chua LL, Friend RH, Ho PKH (2010) High-performance polymer semiconducting heterostructure devices by nitrene-mediated photocrosslinking of alkyl side chains. Nat Mater 9:152
9. Yan H, Lee P, Armstrong NR, Graham A, Evmenenko GA, Dutta P, Marks TJ (2005) High-performance hole-transport layers for polymer light-emitting diodes. Implementation of organosiloxane cross-linking chemistry in polymeric electroluminescent devices. J Am Chem Soc 127:3172
10. Huang F, Niu YH, Zhang Y, Ka JW, Liu MS, Jen AKY (2007) A conjugated, neutral surfactant as electron-injection material for high-efficiency polymer light-emitting diodes. Adv Mater 19:2010
11. Zhang B, Qin C, Niu X, Xie Z, Cheng Y, Wang L, Li X (2010) On the origin of efficient electron injection at phosphonate-functionalized polyfluorene/aluminum interface in efficient polymer light-emitting diodes. Appl Phys Lett 97:043506
12. Zhao Y, Xie Z, Qin C, Qu Y, Geng Y, Wang L (2009) Enhanced charge collection in polymer photovoltaic cells by using an ethanol-soluble conjugated polyfluorene as cathode buffer layer. Sol Energy Mater Sol C 93:604
13. Wu HB, Huang F, Peng JB, Cao Y (2005) High-efficiency electron injection cathode of Au for polymer light-emitting devices. Org Electron 6:118
14. Zhou G, Qian G, Ma L, Cheng YX, Xie ZY, Wang LX, Jing XB, Wang FS (2005) Polyfluorenes with phosphonate groups in the side chains as chemosensors and electroluminescent materials. Macromolecules 38:5416
15. Ma H, Yip H-L, Huang F, Jen AKY (2010) Interface engineering for organic electronics. Adv Funct Mater 20:1371
16. Huang F, Wu H, Cao Y (2010) Water/alcohol soluble conjugated polymers as highly efficient electron transporting/injection layer in optoelectronic devices. Chem Soc Rev 39:2500
17. Hoven CV, Garcia A, Bazan GC, Nguyen T-Q (2008) Recent applications of conjugated polyelectrolytes in optoelectronic devices. Adv Mater 20:3793
18. Hoven CV, Yang RQ, Garcia A, Crockett V, Heeger AJ, Bazan GC, Nguyen TQ (2008) Electron injection into organic semiconductor devices from high work function cathodes. Proc Natl Acad Sci USA 105:12730

19. Chen LM, Xu Z, Hong Z, Yang Y (2010) Interface investigation and engineering—achieving high performance polymer photovoltaic devices. J Mater Chem 20:2575
20. Thomas SW, Joly GD, Swager TM (2007) Chemical sensors based on amplifying fluorescent conjugated polymers. Chem Rev 107:1339
21. Jiang H, Taranekar P, Reynolds JR, Schanze KS (2009) Conjugated polyelectrolytes: synthesis, photophysics, and applications. Angew Chem Int Ed 48:4300
22. Huang F, Wu HB, Wang D, Yang W, Cao Y (2004) Novel electroluminescent conjugated polyelectrolytes based on polyfluorene. Chem Mater 16:708
23. Zhou G, Geng YH, Cheng YX, Xie ZY, Wang LX, Jing XB, Wang FS (2006) Efficient blue electroluminescence from neutral alcohol-soluble polyfluorenes with aluminum cathode. Appl Phys Lett 89:233501
24. Tung RT (2001) Recent advances in Schottky barrier concepts. Mater Sci Eng R 35:1
25. Parker ID, Cao Y, Yang CY (1999) Lifetime and degradation effects in polymer light-emitting diodes. J Appl Phys 85:2441
26. Lee TW, Kim MG, Park SH, Kim SY, Kwon O, Noh T, Park JJ, Choi TL, Park JH, Chin BD (2009) Designing a stable cathode with multiple layers to improve the operational lifetime of polymer light-emitting diodes. Adv Funct Mater 19:1863
27. Choong V, Park Y, Shivaparan N, Tang CW, Gao Y (1997) Deposition-induced photoluminescence quenching of tris-(8-hydroxyquinoline) aluminum. Appl Phys Lett 71:1005
28. Choong V, Park Y, Gao Y, Wehrmeister T, Mullen K, Hsieh BR, Tang CW (1996) Dramatic photoluminescence quenching of phenylene vinylene oligomer thin films upon submonolayer Ca deposition. Appl Phys Lett 69:1492
29. Niu X, Qin C, Zhang B, Yang J, Xie Z, Cheng Y, Wang L (2007) Efficient multilayer white polymer light-emitting diodes with aluminum cathodes. Appl Phys Lett 90:203513
30. Vaynzof Y, Dennes TJ, Schwartz J, Kahn A (2008) Enhancement of electron injection into a light-emitting polymer from an aluminum oxide cathode modified by a self-assembled monolayer. Appl Phys Lett 93:103305
31. Vioux A, Le Bideau J, Mutin PH, Leclercq D (2004) Hybrid organic-inorganic materials based on organophosphorus derivatives. Top Curr Chem 232:145
32. Bardecker JA, Ma H, Kim T, Huang F, Liu MS, Cheng YJ, Ting G, Jen AKY (2008) Self-assembled electroactive phosphonic acids on ITO: maximizing hole-injection in polymer light-emitting diodes. Adv Funct Mater 18:3964
33. Le QT, Yan L, Gao YG, Mason MG, Giesen DJ, Tang CW (2000) Photoemission study of aluminum/tris-(8-hydroxyquinoline) aluminum and aluminum/LiF/tris-(8-hydroxyquinoline) aluminum interfaces. J Appl Phys 87:375
34. Oyamada T, Yoshizaki H, Sasabe H, Adachi C (2004) Efficient electron injection characteristics of triazine derivatives for transparent OLEDs (TOLEDs). Chem Lett 33:1034
35. Huang JS, Xu Z, Yang Y (2007) Low-work-function surface formed by solution-processed and thermally deposited nanoscale layers of cesium carbonate. Adv Funct Mater 17:1966
36. Huang JS, Hou WJ, Li JH, Li G, Yang Y (2006) Improving the power efficiency of white light-emitting diode by doping electron transport material. Appl Phys Lett 89:133509
37. Huang JS, Li G, Wu E, Xu QF, Yang Y (2006) Achieving high-efficiency polymer white-light-emitting devices. Adv Mater 18:114
38. Tang CW, Vanslyke SA (1987) Organic electroluminescent diodes. Appl Phys Lett 51:913
39. Zhang B, Qin C, Ding J, Chen L, Xie Z, Cheng Y, Wang L (2010) High-performance all-polymer white-light-emitting diodes using polyfluorene containing phosphonate groups as an efficient electron-injection layer. Adv Funct Mater 20:2951
40. Liu J, Chen L, Shao SY, Xie ZY, Cheng YX, Geng YH, Wang LX, Jing XB, Wang FS (2007) Three-color white electroluminescence from a single polymer system with blue, green and red dopant units as individual emissive species and polyfluorene as individual polymer host. Adv Mater 19:4224
41. Chen SH, Su AC, Su CH, Chen SA (2005) Crystalline forms and emission behavior of poly(9,9-di-n-octyl-2,7-fluorene). Macromolecules 38:379
42. Kreouzis T, Poplavskyy D, Tuladhar SM, Campoy-Quiles M, Nelson J, Campbell AJ, Bradley DDC (2006) Temperature and field dependence of hole mobility in poly(9,9-dioctylfluorene). Phys Rev B 73:235201
43. Hung LS, Zhang RQ, He P, Mason G (2002) Contact formation of LiF/Al cathodes in Alq-based organic light-emitting diodes. J Phys D 35:103

44. Chen L, Zhang B, Cheng Y, Xie Z, Wang L, Jing X, Wang F (2010) Pure and saturated red electroluminescent polyfluorenes with dopant/host system and PLED efficiency/color purity trade-offs. Adv Funct Mater 20:3143
45. Ma Z, Ding J, Zhang B, Mei C, Cheng Y, Xie Z, Wang L, Jing X, Wang F (2010) Red-emitting polyfluorenes grafted with quinoline-based iridium complex: "simple polymeric chain, unexpected high efficiency". Adv Funct Mater 20:138
46. Brabec CJ, Shaheen SE, Winder C, Sariciftci NS, Denk P (2002) Effect of LiF/metal electrodes on the performance of plastic solar cells. Appl Phys Lett 80:1288
47. Zhao Y, Xie Z, Qu Y, Geng Y, Wang L (2008) Effects of thermal annealing on polymer photovoltaic cells with buffer layers and in situ formation of interfacial layer for enhancing power conversion efficiency. Synth Met 158:908
48. Zhang F, Ceder M, Inganas O (2007) Enhancing the photovoltage of polymer solar cells by using a modified cathode. Adv Mater 19:1835
49. Na S-I, Oh S-H, Kim S-S, Kim D-Y (2009) Efficient organic solar cells with polyfluorene derivatives as a cathode interfacial layer. Org Electron 10:496
50. Luo J, Wu H, He C, Li A, Yang W, Cao Y (2009) Enhanced open-circuit voltage in polymer solar cells. Appl Phys Lett 95:043301
51. Seo JH, Gutacker A, Sun Y, Wu H, Huang F, Cao Y, Scherf U, Heeger AJ, Bazan GC (2011) Improved high-efficiency organic solar cells via incorporation of a conjugated polyelectrolyte interlayer. J Am Chem Soc 133:8416
52. Ye T, Zhu M, Chen J, Ma D, Yang C, Xie W, Liu S (2011) Efficient multilayer electrophosphorescence white polymer light-emitting diodes with aluminum cathodes. Org Electron 12:154
53. Xu XF, Cai WZ, Chen JW, Cao Y (2011) Conjugated polyelectrolytes and neutral polymers with poly(2,7-carbazole) backbone: synthesis, characterization, and photovoltaic application. J Polym Sci Pol Chem 49:1263